

Musculoskeletal Pathology

Molecular Profiling of Giant Cell Tumor of Bone and the Osteoclastic Localization of Ligand for Receptor Activator of Nuclear Factor κ B

Teresa Morgan,* Gerald J. Atkins,[†]
Melanie K. Trivett,[‡] Sandra A. Johnson,*
Maya Kansara,* Stephen L. Schlicht,[§]
John L. Slavin,[§] Paul Simmons,* Ian Dickinson,[¶]
Gerald Powell,[§] Peter F.M. Choong,[§]
Andrew J. Holloway,* and David M. Thomas*

From the Ian Potter Foundation Center for Cancer Genomics and Predictive Medicine and Research Division* and the Department of Pathology,[‡] Peter MacCallum Cancer Center, Melbourne; the Department of Orthopedics and Trauma,[†] University of Adelaide, South Australia; the Departments of Orthopedics, Radiology, and Pathology,[§] St. Vincent's Hospital, Melbourne; and Wesley Hospital,[¶] Brisbane, Queensland, Australia

Giant cell tumor of bone (GCT) is a generally benign, osteolytic neoplasm comprising stromal cells and osteoclast-like giant cells. The osteoclastic cells, which cause bony destruction, are thought to be recruited from normal monocytic pre-osteoclasts by stromal cell expression of the ligand for receptor activator of nuclear factor κ B (RANKL). This model forms the foundation for clinical trials in GCTs of novel cancer therapeutics targeting RANKL. Using expression profiling, we identified both osteoblast and osteoclast signatures within GCTs, including key regulators of osteoclast differentiation and function such as RANKL, a C-type lectin, osteoprotegerin, and the wnt inhibitor SFRP4. After *ex vivo* generation of stromal- and osteoclast-enriched cultures, we unexpectedly found that RANKL mRNA and protein were more highly expressed in osteoclasts than in stromal cells, as determined by expression profiling, flow cytometry, immunohistochemistry, and reverse transcription-polymerase chain reaction. The expression patterns of molecules implicated in signaling between stromal cells and monocytic osteoclast precursors were analyzed in both primary and fractionated GCTs. Finally, using array-based comparative genomic hybridization, neither GCTs nor the derived stromal cells demonstrated significant genomic gains

or losses. These data raise questions regarding the role of RANKL in GCTs that may be relevant to the development of molecularly targeted therapeutics for this disease. (Am J Pathol 2005, 167:117-128)

Giant cell tumors of bone (GCT) are rare, usually benign connective tissue neoplasms characterized by localized bone destruction. They comprise osteoclast-like giant cells, stromal cells, and CD68-positive monocytes.^{1,2} The stromal cells are thought to be the neoplastic component of the tumor, as they can be propagated in culture and stain positive for the proliferation marker, Ki67.² There is evidence that the stromal cells are of the osteoblastic lineage²⁻⁴ and are thought to support the recruitment and formation of mature osteoclasts from precursor cells.⁵ It is the bone resorptive activity of osteoclasts that causes the destructive osteolysis and consequent morbidity seen in GCT.⁶ The molecules that mediate this interaction therefore represent potentially important therapeutic targets.

Osteoclast differentiation and activation is critically dependent on the tumor necrosis factor (TNF) receptor/TNF-like proteins, osteoprotegerin (OPG), and ligand for receptor activator of nuclear factor κ B (RANKL).^{5,7,8} RANKL expression has been observed in GCT-derived stromal cells,⁵ and these cells support osteoclast formation in the RAW264.7 murine monocytic cell line.⁹ These and other observations have led to the widely accepted proposition that the expression of RANKL by the neoplastic stromal cell causes the recruitment of osteoclasts.⁵ Unexpectedly, the expression of RANKL mRNA and

Supported by a National Health and Medical Research Council RD Wright Research Fellowship (RegKey no. 251752 to D.T.) and a research grant from the Cancer Council of Victoria (to D.T.).

Accepted for publication February 28, 2005.

Supplemental material for this article appears on <http://ajp.amjpathol.org>.

Address reprint requests to Dr. David Thomas, Ian Potter Foundation Center for Cancer Genomics and Predictive Medicine, Peter MacCallum Cancer Center, St. Andrews Place, East Melbourne 3002, Victoria, Australia. E-mail: david.thomas@petermac.org.

Table 1. Tumor Type and Numbers of Each Arrayed

Tumor type	No. arrayed
Malignant fibrous histiocytoma	11
Liposarcoma	15
Leiomyosarcoma	9
Synovial cell sarcoma	4
Giant cell tumor of bone	9

protein has been reported in osteoclasts, including GCTs.^{10,11} Perhaps because of methodologic issues affecting immunohistochemical and *in situ* hybridization techniques, these incidental findings have not been widely appreciated, and their significance remains unclear. Because several cell types are involved in the genesis of GCT and a network of 60 proteins are involved in osteoclastogenesis,⁶ elucidating the nature and sources of these molecules is important.

To address this issue, we have undertaken genome-wide transcriptional profiling of GCTs. A number of studies have demonstrated the value of molecular profiling of connective tissue neoplasms in general, shedding light on the molecular identity of subclasses of this heterogeneous group of disorders.¹²⁻¹⁴ Our studies have focused on human GCT within the context of 48 sarcomas. GCTs form a distinct group within soft-tissue sarcomas by unsupervised hierarchical clustering. After supervised clustering, we identified genes reported to be expressed in osteoclasts and osteoblasts. Identification of the molecules that modulate osteoclastogenesis using genetic profiling and functional assays may lead to the discovery of novel therapeutic targets. As expected, RANKL expression was high in GCTs, and its inhibitor (osteoprotegerin) showed low expression. Using *ex vivo* cellular fractionation methods, we generated osteoclast- and stromal cell-enriched fractions and unexpectedly found that RANKL expression was greater in the osteoclast-enriched hemopoietic fraction. This finding was confirmed by reverse transcriptase-polymerase chain reaction (RT-PCR), flow cytometry, and immunohistochemistry, suggesting that the neoplastic component is derived from cells of the osteoclast lineage or that a molecule other than RANKL is responsible for osteoclast recruitment by the stromal cells or that both cell components are derived from a common precursor.

Materials and Methods

Processing of Tumor Samples

Forty-eight primary tumor samples were obtained from the Tissue Bank at The Peter MacCallum Cancer Center and St Vincent's Hospital in Melbourne, Australia and the Princess Alexandra Hospital, Brisbane, Australia (Table 1). Separate Institutional Review Board approval was obtained for the collection of samples. The samples are stored at the tissue bank at The Peter MacCallum Cancer Center. Resected specimens underwent blinded pathological review by a dedicated sarcoma pathologist (JS) to

ensure at least 80% viable tumor content. The samples obtained and arrayed are shown in Table 1.

Preparation of Total RNA from Tumor Tissue

Tumor samples were added to Trizol reagent (1 ml per 25 mg of tissue) and homogenized for 30 seconds. The sample was then extracted in Trizol reagent, purified using the Qiagen RNeasy kit (Qiagen Ltd, Sussex, UK), and quantified by spectrophotometry.

cDNA Synthesis, Transcription, RNA Purification, and Concentration

First-strand synthesis of cDNA was achieved using the Eberwine method.¹⁵ Briefly, total RNA (3 μ g) was reverse transcribed to cDNA using a T7 promoter tagged anchored PolyT primer. Subsequently, second-strand synthesis was achieved using DNA polymerase I (40 U; Promega, Madison, WI), DNA ligase (10 U; Invitrogen, Carlsbad, CA), RNase H (2 U; Invitrogen), dNTP (10 mmol/L each) and 10 \times DNA polymerase I buffer with an incubation at 16°C for 2 hours. The double-stranded cDNA sample was then used as a template in an *in vitro* transcription reaction using a T7 Megascript kit (Ambion, Austin, TX) following the protocol supplied and then purified using an RNeasy column (Qiagen, Doncaster, Victoria, Australia). The sample was dry eluted to 12 μ l using a vacuum centrifuge and quantified using a spectrophotometer.

Probe Preparation and Hybridization

Amplified RNA (4–10 μ g) was indirectly labeled by incorporation of amino allyl dUTP (Sigma, Sydney, Australia) during reverse transcription. The sample was then purified using the Qiagen QIAquick Purification kit as per the protocol provided with the exception that the sample is not eluted but left on the column for the subsequent coupling step.

Cyanine-5 fluorophor (Amersham, Castle Hill, NSW, Australia) was resuspended in 20 μ l of 0.1 mol/L Na bicarbonate buffer and added to the center of the column above for all of the test samples. Cyanine-3 fluorophor was used for a reference sample, which consists of pooled and amplified RNA from 11 human tumor cell lines.^{16,17} A 1-hour incubation of the column (in the dark) was then required. The sample was then eluted with 80 μ l of water and 13,000 rpm for 1 minute. Five volumes of buffer PB (Qiagen QIAquick kit) was added to each sample.

The eluted cyanine-3-coupled reference sample was added to a new Qiagen column, the eluate was discarded, and then the cyanine-5-coupled test sample was applied to the same column. It was washed with buffer PE, and the sample was eluted with buffer EB (Qiagen). A hybridization mix consisting of tRNA, cot-1 DNA, PolydA, and 50 \times Denharts containing herring sperm DNA was added to the eluted sample, and the sample was then

concentrated in a centrifugal evaporator. Standard saline citrate (SSC; 20×) and 100% deionized formamide were added to the sample; it was denatured at 100°C for 3 minutes. Sodium dodecyl sulfate (10%) was then added, and the samples were ready to apply to the slide and hybridize for 14 to 16 hours in a humidified chamber at 42°C. The slides were then placed in 0.5× SSC and 0.01% sodium dodecyl sulfate until the coverslips came off and then incubated a further 1 minute in the same solution. The next wash was in 0.5% SSC for 3 minutes, and the final wash was in 0.06% SSC for 3 minutes. The slides were then centrifuged dry at 800 rpm for 5 minutes.

Microarray Slides and Analysis

All experiments were performed using two-color competitive hybridization of fluorescently labeled cDNA to a glass slide array. The cDNA microarrays used contain 9386 cDNA clones representing almost all named genes and several thousand additional expressed sequence tag clones (Unigene build no. 172). Each test sample was compared with a reference sample consisting of pooled RNA from 11 cell lines. The slides were scanned using an Agilent scanner and analyzed using Genepix Pro 4.1 and Genespring software (Silicon Genetics). The following transformations were applied to the raw data. First, adjustments were made for three dye-swapped GCT samples followed by locally weighted regression scatterplot smoothing normalization, and finally, all data were median normalized for gene expression. Spots flagged as absent in more than 3 of 48 samples were excluded from further analysis, yielding 6822 genes (supplemental data at <http://ajp.amjpathol.org>), and then these genes were filtered on the basis of raw signal (>300), yielding 3376 genes. For supervised hierarchical clustering, we applied Welch's analysis of variance with a *P* value cut-off of 0.05 and Bonferroni's multiple test correction to generate a list of 171 genes that reliably discriminated between histological subtypes (supplemental data at <http://ajp.amjpathol.org>). For experiments using osteoblast- and osteoclast-enriched cultures, filtered data were manually analyzed using Microsoft Excel (supplemental data at <http://ajp.amjpathol.org>).

Array Comparative Genomic Hybridization

DNA was extracted from tumor samples or cell culture using standard protocols.¹⁸ A total of 3 μg of DNA was sent to the Microarray Shared Resource at the Comprehensive Cancer Center, University of California, San Francisco, and subjected to array-based comparative genomic hybridization as previously described.¹⁹

Subfractionation of GCT into Giant Cell and Stromal Fractions

Selected GCT samples were subfractionated according to the method published by Atkins et al.⁵ Briefly, GCT samples were used fresh, treated with collagenase, and

cultured in Dulbecco's modified Eagle's medium containing 10% fetal calf serum. The cultured sample consisted of giant cells in a stromal cell mass. The stromal cell fraction was removed by trypsin digestion (0.1% w/v in phosphate-buffered saline (PBS)) and replated into a separate flask while the giant cells and mononuclear fan-shaped cells remained attached to the flask. After 48 hours, the process was repeated until giant cells were no longer seen in the stromal fraction, yielding a stromal cell-enriched fraction and a giant cell-enriched fraction.

For bioassays of RANKL production, we used RAW264.7 cells, a monocytic cell line that forms osteoclasts in the presence of recombinant human RANKL.²⁰ Briefly, either the supernatants from primary stromal cell cultures were added to RAW264.7 cells or stromal cells were co-cultured with RAW264.7 cells. RAW264.7 cells were then cultured for up to 10 days before staining for tartrate-resistant acid phosphatase (TRAP) as described previously.²⁰ Control cultures were conducted using recombinant human RANKL to ensure that these cells formed TRAP-positive osteoclast like cells.

PCR Samples and Conditions

GCT, osteoblast, and osteoclast cDNAs were diluted 1 in 25, and 1 μL was used for PCR. cDNA was amplified using the PCR primers listed in Table 2 to generate mRNA products encoding the specific human genes. The 25-μL PCR reaction consisted of 1 U of AmpliTaq Gold DNA polymerase (Perkin-Elmer, Norwalk, CT), 0.4 mmol/L dNTPs (Pharmacia Biotech, Uppsala, Sweden), 1.5 mmol/L magnesium chloride, 50 nmol/L of each primer, and 1× PCR buffer and was made to volume with RNase-free water. The conditions used were: 95°C for 5 minutes to activate the polymerase and 40 cycles of 95°C for 30 seconds to denature, 50 to 56°C gradient for 30 seconds to anneal, and 72°C for 30 seconds for extension; the 40 cycles were followed by an additional extension of 72°C for 5 minutes, and then the samples were kept at 4°C before the addition of loading buffer (6×). They were then run on a 1.8% agarose gel and visualized via ethidium bromide staining.

PCR Primers

Some of the primer sequences used were obtained from Atkins et al,⁵ whereas the remainder were generated from sequences corresponding to accession numbers for cDNAs contained in our microarrays.

Flow Phenotyping

Fresh GCT samples were collagenase treated as described above. Cells were disaggregated and passed through a 19-gauge needle to remove debris. All subsequent steps were carried out at 4°C. Cells were incubated with PerCP-conjugated monoclonal anti-human CD45 (DAKO) for 15 minutes, followed by washing (PBS and 1% bovine serum albumin). After fixation in 2% paraformaldehyde for 10 minutes on ice, cells were incubated with monoclonal anti-human RANKL (MAB626; R&D Systems) at 1 μg/ml for 10

Table 2. Primers to Osteoclast, Osteoblast, and Giant Cell Tumor Markers Selected through Microarray Expression Signatures as well as Published Data⁵

Target gene	Sense (5' to 3')	Antisense (5' to 3')	Melting temperature (°C)	Product (bp)
OPG	TGCTGTTCTACAAAGTTTACG	CTTTGAGTGCTTTAGTGCGTG	62	435
M-CSF	CAGTTGTCAAGGACAGCAC	GCTGGAGGATCCCTTCGGACTG	58	670
SFRP4	TGCTGCCGACTGGAGTTTG	TGAGGTCCCACGTTTACCC	63	529
RANKL	AATAGAATATCAGAAGATGGCACTC	TAAGGAGGGGTTGGAGACCTCG	62	668
C-type lectin	TCCAGGCTGTCTCTCCACG	TGTGCCTATCTGGTGCCTCTG	65	557
CTR	GCAATGCTTTCACTCCTGAGAAA	AGTGCATCACGTAATCATATATC	58	782
TRAP	CTGGCTGATGGTGCCACCCCTG	CTCTCAGGCTGCAGGCTGAGG	65	469
CSF1R	GCTTGGCATGGTCAGGGAAT	GGGCCCTGGGATGACTTTCT	65	898
Cathepsin K	GATCACTGGAGCTGACTTCCG	GGGCTCTACCTTCCCATTCTG	66	470
OSF1	TCCTAGGAGGCGACGGTTGT	CGTGGCAAGCCCAGTATAAGG	63	495
OSF2	GGACCAAGGCCCAAATGTCT	CCCATGGATGATTCGAGCA	63	653
Osteonectin	GCAAGAAGCCCTGCCTGAT	GGGAATTCGGTCAGCTCAGA	62	548
GAPDH	CACTGACACCTTGGCAGTGG	CATGGAGAAGGCTGGGGCTC	60	414

minutes. After washing, cells were blocked in PBS containing 10% mouse serum for 10 minutes on ice. After three more washes, cells were incubated with fluorescein isothiocyanate (FITC)-conjugated donkey anti-mouse immunoglobulin (Jackson ImmunoResearch) for 10 minutes before three washes in PBS/bovine serum albumin. Appropriate negative controls were included. Cells were then subject to flow cytometry (FACScalibur, Becton Dickinson).

Immunohistochemistry

Paraffin-embedded tissue sections were cut and mounted onto slides. These were stained with TRAP using an alkaline leukocyte phosphatase kit (Sigma), CD68 antibody, CD45 antibody, CD4 antibody, RANKL antibody, and vimentin. Immunostaining for RANKL was performed using the same antibody described above (MAB626).

Results and Discussion

Expression Profiling of Giant Cell Tumor of Bone

We undertook expression profiling of 48 sarcomas, including 9 GCTs. Using unsupervised hierarchical clustering, GCTs formed a distinct subgroup, consistent with the striking morphology of these tumors (Figure 1A). Supervised clustering (Figure 1B), based on genes that accurately discriminated between subclasses of sarcomas ($P < 0.01$), reinforced the impression that GCTs formed a remarkably homogeneous subgroup. A full discussion of the remaining classes of sarcoma lies beyond the scope of this paper, but the raw data are provided as supplemental information (<http://ajp.amjpathol.org>). We next examined those genes most highly expressed in GCTs, ranked according to their median expression (Table 3). This gene list comprises the top 20 genes and their median expression in GCTs. As expected, the list included several genes known to be highly expressed in osteoclasts, including cathepsin K²¹, the brain isoform of creatine kinase,²² calcineurin-dependent nuclear factor of activated T-cells,²³ and subunit of a membrane-associated ATP-dependent proton pump.²⁴ Additionally, a number of osteoblast-related genes were iden-

tified, including decorin, lumican, and collagen IX, consistent with the proposition that the stromal element in GCTs is of osteoblastic origin. Almost all remaining genes identified in our study have been implicated in osteoclast biology. Foremost among these, RANKL (tumor necrosis factor superfamily member 11) was extremely highly expressed in these tumors, whereas OPG was expressed at very low levels (data not shown). Because OPG is a decoy inhibitor of RANKL signaling, this is consistent with a potent osteoclastogenic signal in GCTs. C-type lectin (member 6) belongs to a class of molecules previously identified as inhibitors of osteoclast formation (osteoclast-inhibitory lectin).²⁵ C-type lectin 6 and murine osteoclast-inhibitory lectin are 23% identical and 51% similar at the protein level, suggesting overlapping functions. Similarly, SFRP4 belongs to a family of secreted frizzled-related proteins, one of which (SFRP1) has aroused interest as an inhibitor of osteoclastogenesis.^{26,27} It is not clear whether C-type lectin 6 or SFRP4 are acting as inhibitors or activators of osteoclast formation in GCTs, because homologs may act in an antagonistic function, as seen with OPG and RANKL. Decysin 1 is a member of the ADAM family (a disintegrin and metalloprotease), which has been implicated in regulation of osteoclast recruitment and function.²⁸ Protein kinase A mediates signals downstream of a number of osteoclastogenic stimuli, including parathyroid hormone and prostaglandins.^{29,30} Lymphotoxin- β receptor binds and transduces signals from tumor necrosis factor family proteins, to which RANKL and OPG belong.^{31,32} Thrombospondin-1 has been reported to stimulate bone resorption by osteoclasts *in vitro*³³, whereas there have been two studies indicating that TYRO3 and its ligand, GAS6, stimulate osteoclast bone resorption.^{34,35} Our studies provide strong evidence that these molecules, which are expressed at high levels in GCTs, play key roles in osteoclast recruitment and function in human disease.

Molecular Profiling of Stromal- and Osteoclast-Enriched Fractions of GCT

We sought to confirm the stromal origin of RANKL in GCTs by fractionating the stromal and hemopoietic com-

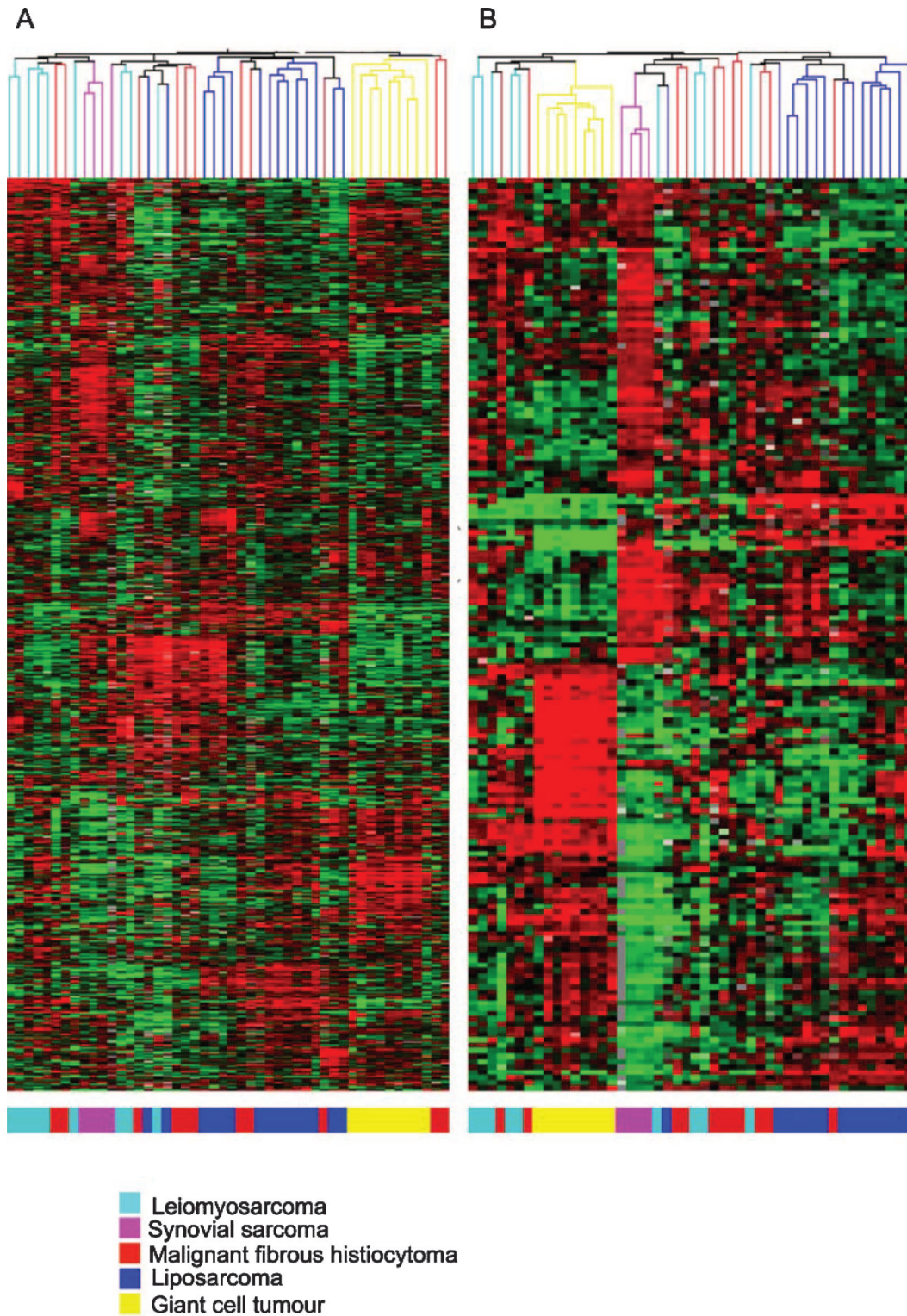


Figure 1. Gene expression heatmaps for leiomyosarcoma, synovial sarcoma, malignant fibrous histiocytoma, liposarcoma, and giant cell tumor using both unsupervised (A) and supervised (B) analysis.

ponents, followed by expression profiling of the stromal-enriched and hemopoietic-enriched cultures.⁵ This crude fractionation procedure resulted in isolation of relatively pure populations of stromal cells, but osteoclast-enriched populations tended to demonstrate residual stromal cell

contamination, probably reflecting the nature of the purification process (Figure 2, A and B). Gene expression signatures were obtained that reflect relative enrichment in osteoclast and osteoblast-like cellular components of GCT (Figure 3 and Table 4). Specifically, we observed

Table 3. Top 24 Genes Most Highly Expressed in Giant Cell Tumor of Bone by Microarray Analysis

Class	Gene name	Accession no.	Median gene expression
Stromal phenotype genes	Matrix metalloproteinase 13 (collagenase 3)	N69322	63
	Decorin	H64138	56
	Collagen type XI α 1	R52907	51
	Collagen, type I, α 2	AA490172	18
	Lumican	AA447781	32
Osteoclast phenotype genes	Collagen, type V, α 1	R75635	21
	Cathepsin K (pyncnodysostosis)	R00859	74
	Acid phosphatase 5, tartrate resistant	R08817	36
	Creatine kinase, brain	AA894557	34
	Thymidine kinase 1, soluble	AA778098	18
	Nuclear factor of activated T-cells, c1	AA679278	24
	Colony stimulating factor 1 receptor	AA284954	23
	ATPase, H ⁺ transporting, lysosomal V0 protein a isoform 3	AI359884	19
Osteoclast regulatory genes	Thrombospondin 2 precursor	H38240	50
	TNF superfamily, member 11 (RANKL)	AA504211	42
	Secreted frizzled-related protein 4	AA487193	41
	C-type lectin, superfamily member 6	AA677149	32
Unknown role	<i>Homo sapiens</i> cDNA clone IMAGE:122159 3', mRNA sequence	T98612	38
	Hypothetical protein, estradiol-induced	R36989	26
	TYRO protein tyrosine kinase binding protein	H12338	24
	<i>H. sapiens</i> cDNA clone IMAGE:51447 3', mRNA sequence	H20822	23
	lymphotoxin- β receptor (TNFR superfamily, member 3)	AA454646	20
	Vanin 1	AA983530	19
	Coagulation factor XIII, A1 polypeptide	AA449742	18

relative enrichment in the osteoclastic fraction of markers known to be highly expressed in monocytes and osteoclasts (cathepsin K, CD4, CD68, ATP-dependent proton pump subunits, and α V integrin) and relative depletion in stromal or osteoblastic genes (decorin, collagens, and lumican). Notable among genes enriched in the osteoclast fraction is the microphthalmia transcription factor (Mitf) family member, TFEC. Mice deficient in *mitf*, the canonical member of the Mitf family, closely resemble mice lacking cathepsin K and have dysfunctional osteoclasts leading to osteopetrosis.³⁶ Although *Tfec*-deficient mice appear phenotypically normal, Mitf, TFEB, TFEC, and TFE3 are functionally redundant basic helix-loop-helix-leucine zipper transcription factors that form homo- and heterodimeric complexes on DNA and have been shown to regulate expression of cathepsin K.³⁷ Our data suggest that TFEC plays an important role in human osteoclast biology. Another highly enriched protein in the osteoclast-enriched fraction is GRB2-binding protein, previously reported to be abundant in osteoclasts,³⁸ and cystatin B, which is found in osteoclasts and may regulate cathepsin activity.³⁹ The stromal fraction expressed osteoblastic or mesenchymal cell markers, including fibroblast growth factor receptor 1, osteoglycin, lumican, collagen XI, and decorin.

Expression of RANKL Is Enriched in the Osteoclast Fraction

Unexpectedly, we observed striking segregation of signaling molecules with known or potential roles in osteoclast differentiation and function in the osteoclast-enriched fraction, including RANKL, SFRP4, and C-type lectin 6 (Figure 3 and Table 4). In contrast, we observed

slight relative enrichment of the osteoblastic fraction for the inhibitor of osteoclastogenesis, OPG. To confirm this result, we undertook semiquantitative RT-PCR for osteoblast and osteoclast markers, as well as regulators of

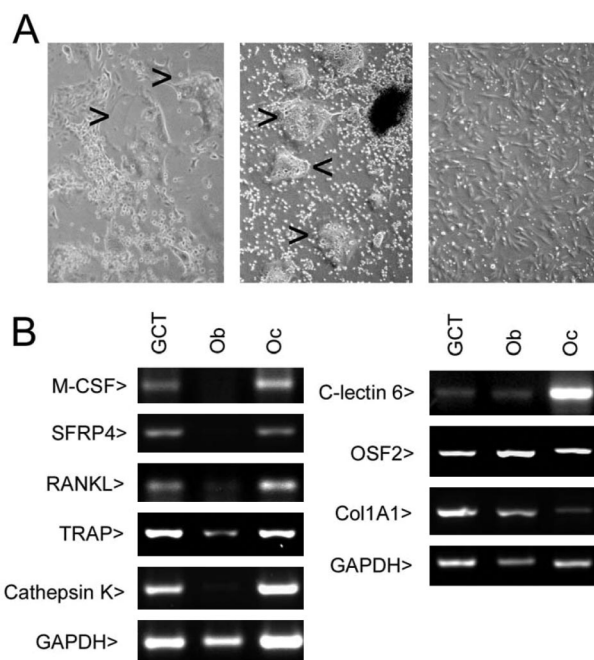


Figure 2. Cell fractionation studies. **A:** Light microscopy showing typical cultures of primary disaggregated giant cell tumor (GCT; left panel), osteoclast-enriched cultures (middle panel), and stromal cell cultures (right panel). Arrows indicate giant cells. **B:** RT-PCR for expression of regulatory genes, osteoclast and osteoblast markers in primary giant cell tumor cultures, and osteoblast- and osteoclast-enriched fractions of GCT. This experiment was performed three times with similar results using independent samples to those used in Table 4.

OC-enriched genes	Stromal cell enriched genes
transcription factor EC	melanoma antigen, family A, 4
colony stimulating factor 1 receptor	transcriptional co-repressor of retinoid and thyroid hormone action (SMRT)
S100 calcium binding protein A3	Collagen type XI alpha 1
GRB2-associated binding protein 1	collagen, type I, alpha 2
KIAA1199 protein	extracellular matrix protein 2, female organ and adipocyte specific
solute carrier family 22 (organic cation transporter), member 1	decorin
nuclear factor of activated T-cells, calcineurin-dependent 1	endothelial differentiation, sphingolipid G-protein-coupled receptor, 1
regulator of G-protein signalling 1	hypothetical protein, estradiol-induced
tumor necrosis factor (ligand) superfamily, member 11	H factor (complement)-like 1
C-type lectin, superfamily member 6	lumican
ribonuclease, RNase A family, k6	phospholipase A2 receptor 1, 180kDa
selectin P ligand	BASIC FIBROBLAST GROWTH FACTOR RECEPTOR 1 PRECURSOR
chemokine (C-C motif) receptor 1	complement component 1, r subcomponent
CD4 antigen (p55)	TSHUP2 thrombospondin 2 precursor - human
adenylate kinase 5	KIAA0471 gene product
A kinase (PRKA) anchor protein 3	ectonucleotide pyrophosphatase/phosphodiesterase 2 (autotaxin)
regulator of G-protein signalling 10	PDZ domain containing 3
CYSTATIN B (HUMAN);, mRNA sequence.	epithelial membrane protein 1
ATPase, H+ transporting, lysosomal V0 protein a isoform 3	fibroblast activation protein, alpha
potassium voltage-gated channel, subfamily F, member 1	coagulation factor XIII, A1 polypeptide
lymphocyte-specific G protein-coupled receptor)	osteoglycin (osteoinductive factor, mimecan)
creatine kinase, brain	MASP-2 PROTEIN. ;, mRNA sequence.
ubiquitin fusion degradation 1-like	integrin, beta-like 1 (with EGF-like repeat domains)
hypothetical protein DKFZp434L142	
potassium channel, subfamily K, member 7	
CDC20 cell division cycle 20 homolog (S. cerevisiae)	
cathepsin K (pyncnodysostosis)	
secreted frizzled-related protein 4	
dermatan sulfate proteoglycan 3	
Homo sapiens cDNA FLJ10130 fis, clone HEMBA1003035.	
chondroadherin	
ATPase, H+ transporting, lysosomal 56/58kDa, V1 subunit B, isoform 2	
CYSTATIN B (HUMAN);, mRNA sequence.	

Figure 3. Tabular representation of genes most highly expressed in osteoclast- and stromal cell-enriched fractions of giant cell tumor of bone. Genes highlighted in red are genes reported to be expressed in osteoclasts; in blue, expressed in stromal cells; in green, genes implicated in signaling of osteoclast formation or function (see text for details).

osteoclast formation. As noted above, these data suggest that we have obtained relatively pure populations of stromal cells, whereas the osteoclast-enriched populations contained significant numbers of residual stromal cells (Figure 2, A and B). Consistent with the expression profiling data, the expression of RANKL, SFRP4, and C-type lectin 6 again segregated with markers of the osteoclast phenotype, and these molecules were almost undetectable in the stromal cell-enriched fraction (Figure 2B). This experiment has been repeated three times with similar results. We confirmed these semiquantitative PCR results using real-time quantitative PCR on an independent set of cultures, demonstrating the highest levels of expression of RANKL in unfractionated GCT (relative expression, 3.6, normalized to cystatin A), with intermediate signal in the osteoclast fraction (0.58) and the lowest in the osteoblast fraction (0.08).

As a final assay for RANKL as a secreted or membrane-bound signal mediating the recruitment of monocytic cells by stromal cells, we used RAW264.7 cells as a bioassay for RANKL production. RAW264.7 cells form TRAP-positive mono- and multinucleated osteoclast-like cells in the presence of recombinant human RANKL (in our hands, between 10 and 50 TRAP-positive cells/high-power field²⁰). However, in repeated experiments, neither GCT stromal cell supernatants nor co-culture with GCT-derived stromal cells resulted in the formation of TRAP-positive cells (data not shown). These data support the view that primary cultures of GCT-derived stromal cells do not secrete or express at the cell surface biologically significant levels of RANKL.

In Situ RANKL Expression in GCTs

Given the presence of contaminating stromal cells in the osteoclast-enriched fraction, we could not exclude the possibility that RANKL expression occurred in stromal cells, but only in the presence of osteoclast-like cells. To test this possibility, we undertook two experiments examining RANKL expression *in situ*. First, we undertook a flow cytometric study of disaggregated GCTs, specifically examining co-expression of CD45 (a pan-hemopoietic marker) and RANKL. We found that CD45 was expressed on osteoclasts in GCTs, along with high levels of CD68 and low levels of CD4, consistent with the hemopoietic origin of these cells. We found that approximately 50% of CD45-positive cells expressed RANKL, whereas we were unable to detect significant expression of RANKL on CD45-negative cells (Figure 4). Second, we immunostained GCTs for RANKL, CD4, CD45, and CD68. These markers were chosen because CD4 and CD68 were observed to be expressed in the osteoclast fraction (Table 4; data not shown), and CD45 is a pan-leukocyte marker consistent with the hemopoietic origin of osteoclasts. Giant cells stained for CD4 and CD45 at the plasma membrane and for CD68 in the cytoplasm (Figure 5), as well as tartrate-resistant acid phosphatase (data not shown). By contrast, these markers were absent from stromal cells within these tumors, which stained strongly with vimentin (data not shown). RANKL immunoreactivity was noted most strongly surrounding osteoblasts adjacent to newly forming bone at the periphery of the GCT (Figure 6, A and B) and in giant cells in these studies

Table 4. Genes Encoding Cytokines or Receptors Found Overexpressed (Greater Than 2-fold Enriched) in Either Primary GCTs or Osteoblast-Enriched or Osteoclast-Enriched Cell Populations

	Accession No.	Median expression in osteoblast-enriched population	Median expression in osteoclast-enriched population	Relative median expression	Unigene name
Giant cell tumor	AA036881			5.56	Chemokine (C-C motif) receptor 1
	AA437226			2.63	Interleukin 10 receptor, α
	N54821			2.51	Interleukin 2 receptor, γ
Osteoclast-enriched	AA449440			2.37	Interferon- γ receptor 2
	AA504211	3.42	45.06	13.18	TNF member 11 (RANKL)
	AA150507	0.96	7.56	7.88	Interleukin 1, β
	AA779457	1.11	8.12	7.32	Bone morphogenetic protein 5
	AI569017	1.24	7.55	6.08	Bone morphogenetic protein 2
	AW073000	1.71	9.33	5.45	TNF receptor member 14
	N54821	0.43	1.74	4.08	Interleukin 2 receptor, γ
	AA936768	1.22	3.77	3.10	Interleukin 1, α
	AA463225	0.42	0.10	4.06	Bone morphogenetic protein 4
	Osteoblast-enriched	AA194983	0.44	0.14	3.20
AA253464		0.45	0.16	2.41	Dickkopf 1
W73473		0.42	0.18	2.39	Bone morphogenetic protein 7
AA490494		1.11	0.47	2.34	TNF receptor member 21
AA464525		6.14	2.70	2.27	Interleukin 1 receptor, type I
AA456160		1.10	0.50	2.19	Fibroblast growth factor receptor 2
W15390		1.38	0.63	2.18	Bone morphogenetic protein receptor IA

Note that relative median expression indicates expression relative to remaining sarcoma types for primary GCT and expression relative to noncognate population for osteoblast- and osteoclast-enriched populations.

(Figure 6, C to F). There was little RANKL staining in the mononuclear population in the bulk of the GCT. Interestingly, the pattern of RANKL staining was not membrane associated (for comparison, see CD45 and CD4 staining in Figure 5, B and C). Taken together, these data suggest that RANKL mRNA and protein are expressed by osteoclasts within GCTs. RANKL is also detectable in some stromal cells, although it appears that levels are depleted in isolated stromal cell populations. The progressive loss of expression of RANKL and osteoblast markers by the isolated stromal fraction raises the possibility that there may be reciprocal interactions between the stromal cell and the osteoclast that support not only osteoclast formation, but maintenance of the osteoblast phenotype. The highest levels of RANKL expression appeared to arise at the margins of the tumor where new bone formation was most evident.

Other Molecules Involved in Stromal-Hemopoietic Cell Signaling

In addition to those described above, several molecules have been implicated in signaling between stromal cells and osteoclast progenitors (reviewed by Boyle et al⁴⁰). Pro-resorptive factors include monocyte colony stimulating factor, interleukins-1, -6, and -11, tumor necrosis factor- α , 1,25(OH)₂ vitamin D₃, parathyroid hormone, and parathyroid hormone-like protein, prolactin, corticosteroids, oncostatin M, and leukemia inhibitory factor. Anti-resorptive factors include platelet-derived growth factor, bone morphogenetic proteins 2 and 4, calcitonin,

estrogens, thrombopoietin, and transforming growth factor- β . Molecules involved in regulation of stromal osteoblast differentiation and function include fibroblast growth factors⁴¹ and bone morphogenetic proteins (BMPs).⁴² We systematically examined expression in GCTs and in the isolated cell populations of these and other genes (Table 4). In many cases, the genes were not represented on the arrays or were removed during filtering because of low expression. Of the remaining 6822 genes, we observed overexpression of the chemokine receptor 1 (CCR1) in primary GCT. CCR1 is a seven-transmembrane G protein-coupled receptor involved in monocyte and macrophage function. Ligands that bind CCR1, including RANTES, macrophage inhibitory protein- α , and monocyte chemotactic protein-3, have been reported to

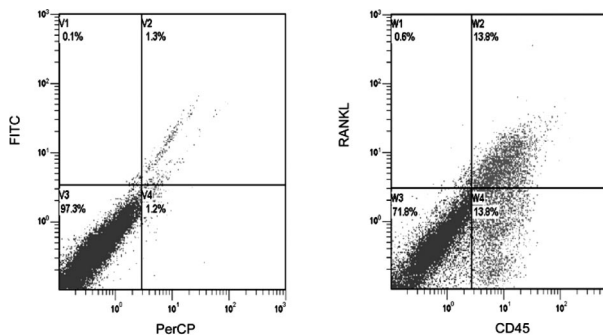


Figure 4. Flow phenotyping of GCT with FITC and PerCP (controls) and RANKL and CD45. There is an increase in the cell population staining positive for both RANKL and CD45, and there are no cells staining RANKL positive and CD45 negative compared with the control samples with FITC and PerCP.

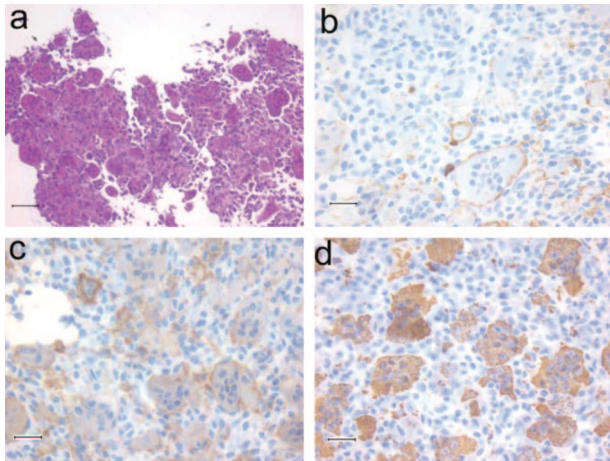


Figure 5. Confirmation of expression profiling data by immunohistochemistry of paraffin-embedded fixed giant cell tumor of bone. **a:** Conventional H&E section; **b:** CD4 staining for osteoclasts; **c:** CD45, which can be also used as an osteoclast cell surface marker; and **d:** CD68, which is a hemopoietic cell or osteoclast marker. Bar = 50 μ m in **a**, and 25 μ m in **b** to **d**.

promote osteoclast differentiation and motility.⁴³ We observed modestly increased expression of receptors for interleukins-2 and -10, and interferon- γ (Table 4). Interestingly, we did not observe increased expression of the ligands for these receptors, although in many cases, these were not represented in our dataset.

In the isolated cell cultures, expression of RANKL dominates the list of signaling molecules in osteoclast-enriched cultures, whereas osteoprotegerin expression was

relatively enriched in the stromal cell fraction (Table 4). Interestingly, interleukin 1- β and - α were relatively overexpressed in the osteoclast-enriched cultures. Interestingly, we also observed relative enrichment for BMP-5 and BMP-2 in osteoclastic populations, whereas the stromal cell-enriched cultures were relatively enriched for the type 1A BMP receptor. This is consistent with reciprocal signaling from the hemopoietic compartment to the stromal compartment. Tian et al⁴⁴ postulated that the elaboration of the Wnt signaling pathway inhibitor, dickkopf 1, may maintain osteoblasts in an immature state, in which expression of RANKL is increased.⁴⁵ dickkopf 1 is not relatively overexpressed in primary GCT (median expression = 1 relative to other sarcomas) but is relatively enriched in the stromal cell fraction. Other molecules involved in regulating stromal cell differentiation and function expressed at higher levels in stromal cells than the osteoclastic fraction included BMP-4 and -7 and the type 2 receptor for fibroblast growth factor.

Conclusions

The observation that RANKL mRNA and protein are highly expressed in osteoclasts in GCT of bone is significant, because they are not consistent with the prevailing pathogenetic model of GCTs.⁴⁶ This holds that the osteoclast component of GCTs is passively recruited by the production of RANKL by the stromal neoplastic component,⁹ based on studies that have shown clearly RANKL expression in GCT stromal cells, and that these cells are capable, when stimulated appropriately, of supporting the formation of osteoclasts.⁵ RANKL is necessary and sufficient for the generation of osteoclasts from monocytic precursors, because the genetic deletion of RANKL results in failure of osteoclastogenesis, and RANKL will substitute for the requirement of stromal cells in co-culture models of osteoclastogenesis.^{8,47} However, a number of observations are difficult to reconcile with this model. Close inspection of data from several studies confirms both RANKL mRNA and protein expression have been detected in osteoclasts, including multinucleated giant cells in GCTs or the related osteoclast-enriched tumor, pigmented villonodular synovitis,^{10,11,48,49} although surprisingly this observation was commented on only in one paper. Moreover, inoculation of GCT-derived stromal cells into SCID mice generated mineralized bone without an excess of osteoclasts or evidence of osteolysis, consistent with an osteoblastic origin, but not inherent osteoclastogenic properties.⁴

How good is the evidence that the stromal component of GCT represents the neoplastic element? First, GCT belongs to a class of benign tumor characterized by a giant cell component, including aneurysmal bone cyst, pigmented villonodular synovitis, and giant cell tumor of tendon sheath.⁴⁶ In these tumors, the giant cell element is usually the minor component, and the histological appearance of the tumor is dominated by the stromal element. In many cases, the giant cell component may be difficult to identify. Second, the stromal element is more readily cultured *ex vivo*, although interestingly monocytic

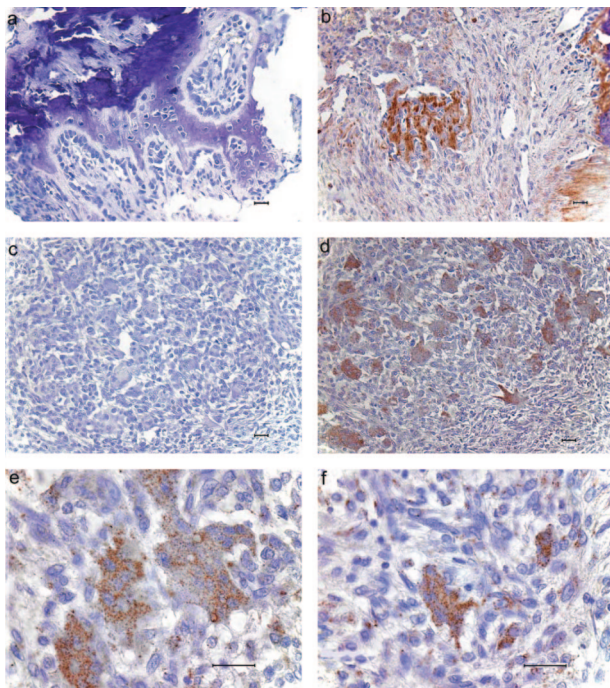


Figure 6. RANKL antibody staining of giant cell tumor of bone. Antibody control GCT section (**a**) and RANKL antibody staining in parallel sections (**b**) showing specific staining adjacent to osteoblasts clustering at a site of newly forming bone. Antibody control (**c**) and RANKL staining (**d**) of parallel sections from a tumor showing specific staining of osteoclasts (low magnification). **e** and **f:** Higher magnification of RANKL-stained osteoclasts, showing granular cytoplasmic staining. Scale bar = 25 μ m.

or osteoclast-like cell lines have successfully been derived from GCT.^{50,51} These lines are capable of spontaneously generating osteoclast-like cells, suggesting that they autonomously possess all of the molecular signals required for osteoclastogenesis, consistent with the expression of RANKL by the hemopoietic component. We are not aware of stromal cell-derived cell lines that have been generated from GCT. Third, several studies have reported clonal karyotypic abnormalities in the stromal cells derived from GCT. The most frequent genetic event observed has been telomeric fusions, with scattered reports of other abnormalities. Telomeric fusions or associations are thought to represent noncovalent interactions at chromosomal ends, and their significance in cancer is fully understood. A reduction in telomere length (average loss of 500 bp) has been reported in giant cell tumor cells when compared with leukocytes from the same patients.⁵² The telomeres commonly affected by fusions include 11p, 13p, 14p, 15p, 19q, 20q, and 21p.⁵³⁻⁵⁷ By contrast, the osteoclast-like cell line, UISO-GCT-1, demonstrated a hypodiploid, hypotetraploid, and multiploid karyotype.⁹ There is a lack of good karyotypic data on the osteoclast-like cells derived from GCTs, in large part due to the difficulty in *ex vivo* culture required for generation of metaphase spreads. We have undertaken ploidy studies using flow cytometry of disaggregated GCTs, and we have not observed an aneuploid population (data not shown). To identify smaller scale recurrent gains or losses, we have used array-based comparative genomic hybridization to examine a limited number of GCTs and the derived stromal cell populations. We did not observe any evidence of deletions or amplified regions in either the primary GCT or the stromal populations (data not shown). These data suggest that the neoplastic fraction within GCTs is not characterized by gross disturbances to genomic integrity. Proof that either the stromal or giant cell compartment (or both) of GCT is neoplastic will come from the demonstration of pathognomonic mutations, and it is likely that these will be subtle.

In summary, our observations are inconsistent with the currently accepted model that the simple elaboration of RANKL by neoplastic stromal cells causes the formation of osteoclast-like cells in GCTs.⁴⁶ There appear to be three alternative interpretations. First, it is possible that RANKL is a necessary downstream effector of osteoclast formation, induced in both stromal and hemopoietic populations by neoplastic stromal cell expression of an unidentified molecule. This model represents a variation of the existing model, positing that the stromal cell still drives osteoclast formation, but that RANKL expression is part of the mechanism rather than the initiating signal. Second, it remains formally possible (although unlikely) that the neoplastic component of the GCT is derived from the hemopoietic compartment, driving osteoclast formation by autocrine stimulation by RANKL. The stromal component may represent the abortive attempt by reactive stromal osteoblasts to repair the bone destruction caused by the neoplastic hemopoietic component. Finally, an unknown common precursor could give rise to all of the cellular elements of GCTs. This intriguing possibility postulates that the neoplastic precursor pos-

esses the ability to manifest both stromal and osteoclastic phenotypes. There is a precedent in biphasic synovial sarcoma, in which both epithelial and stromal elements are demonstrable.⁴⁶ In this model, aberrant expression of RANKL stimulates, in an autocrine/paracrine manner, the stochastic commitment to expression of markers of the osteoclast lineage. Although much work may be required to dissect these alternatives, it is important to determine whether the expression of RANKL is necessary to the formation of osteoclast-like cells, because novel inhibitors of RANKL signaling are being considered as potential therapeutic agents in this otherwise chemo-refractory disease.

Acknowledgments

We thank Lisa Devereux, the Peter Mac Tumor Bank, and members of the Bowtell and Holloway laboratories for helpful discussions.

References

1. Golding SR, Roelke MS, Petrisson KK, Bhan AK: Human giant cell tumor of bone: identification and characterisation of cell types. *J Clin Invest* 1987, 79:483-491
2. Wullung M, Kaiser E: The origin of the neoplastic stromal cell in giant cell tumor of bone. *Hum Pathol* 2003, 34:983-993
3. Joyner CJ, Quinn JM, Triffitt JT, Owen ME, Athanasou NA: Phenotypic characterisation of mononuclear and multinucleated cells of giant cell tumor of bone. *Bone Miner* 1992, 16:37-48
4. James IE, Dodds RA, Olivera DL, Nuttall ME, Gowen M: Human osteoclastoma-derived stromal cells: correlation of the ability to form mineralized nodules *in vitro* with formation of bone *in vivo*. *J Bone Miner Res* 1996, 11:1453-1460
5. Atkins GJ, Hayes DR, Graves SE, Evadokiou A, Hay S, Bouralexis S, Findlay DM: Expression of osteoclast differentiation signals by stromal elements of giant cell tumors. *J Bone Miner Res* 2000, 15:640-649
6. Boyle WJ, Simonet SW, Lacey DL: Osteoclast differentiation and activation. *Nature* 2003, 423:337-342
7. Simonet WS, Lacey DL, Dunstan CR, Kelley M, Chang MS, Luthy R, Nguyen HQ, Wooden S, Bennett L, Boone T, Shimamoto G, DeRose M, Elliot R, Colombero A, Tan HL, Trail TM, Sullivan J, Davy E, Eucay N, Renshaw-Gegg L, Hughes TM, Hill D, Pattison W, Campbell P, Sander S, Van G, Tarpley J, Derby P, Lee R, Boyle WJ: Osteoprotegerin: a novel secreted protein involved in the regulation of bone density. *Cell* 1997, 89:309-319
8. Yasuda H, Shima N, Nakagawa N, Yamaguchi K, Kinoshita M, Mochizuki S, Tomoyasu A, Yano K, Goto M, Murakami A, Tsuda E, Morinaga T, Higashio K, Udagawa N, Takahashi N, Suda T: Osteoclast differentiation factor is a ligand for osteoprotegerin/osteoclastogenesis inhibitory factor and is identical to TRANCE/RANKL. *Proc Natl Acad Sci USA* 1998, 95:3597-3602
9. Huang L, Xu J, Wood DJ, Zheng MH: Gene expression of osteoprotegerin ligand, osteoprotegerin, and receptor activator NF- κ B in giant cell tumor of bone. *Am J Pathol* 2000, 156:761-767
10. Kartsogiannis V, Zhou H, Horwood NJ, Thomas RJ, Hards DK, Quinn JMW, Niforas P, Ng KW, Martin TJ, Gillespie MT: Localisation of RANKL (receptor activator of NF κ B ligand) mRNA and protein in skeletal and extraskeletal tissues. *Bone* 1999, 25:525-534
11. Roux S, Amazit L, Meduri G, Guiochon-Mantel A, Milgrom E, Mariette X: RANK (receptor activator of nuclear factor kappa B) and RANKL ligand are expressed in giant cell tumors of bone. *Am J Clin Pathol* 2002, 117:210-216
12. Khan J, Wei JS, Ringner M, Saal LH, Ladanyi M, Westermann F, Schwab M, Antonescu C, Peterson C, Meltzer PS: Classification and

- diagnostic prediction of cancers using gene expression profiling and artificial neural networks. *Nat Med* 2001, 7:673–678
13. Nielsen TO, West RB, Linn SC, Alter O, Knowling MA, O'Connell JX, Zhu S, Fero M, Sherlock G, Pollack JR, Brown PO, Botstein D, van de Rijn M: Molecular characterisation of soft tissue tumors: a gene expression study. *Lancet* 2002, 359:1301–1307
 14. Segal NH, Pavlidis P, Antonescu CR, Maki RG, Noble WS, DeSantis D, Woodruff JM, Lewis JJ, Brennan MF, Houghton AN, Cordon-Cardo C: Classification and subtype prediction of adult soft tissue sarcoma by functional genomics. *Am J Pathol* 2003, 163:691–700
 15. Van Gelder RN, von Zastrow ME, Yool A, Dement DC, Barchas JD, Eberwine JH: Amplified RNA synthesized from limited quantities of heterogeneous cDNA. *Proc Natl Acad Sci USA* 1990, 87:1663–1667
 16. Pollack JR: RNA common reference sets. *DNA Microarrays: A Molecular Cloning Manual*. Edited by DDL Bowtell, J Sambrook. Cold Spring Harbor, NY, Cold Spring Harbor Press, 2002, pp 168–172
 17. Pollack JR, Sorlie T, Perou CM, Rees CA, Jeffrey SS, Lonning PE, Tibshirani R, Botstein D, Borresen-Dale AL, Brown PO: Microarray analysis reveals a major direct role of DNA copy number alteration in the transcriptional program of human breast tumors. *Proc Natl Acad Sci USA* 2002, 99:12963–12968
 18. Strauss WM: Preparation of genomic DNA from mammalian tissue. *Current Protocols in Molecular Biology*. Edited by FM Ausubel, R Brent, RE Kingston, DD Moore, JA Smith, JG Seidman, S Struhl. New York, John Wiley & Sons, 1990, pp 2.2.1–2.2.3
 19. Snijders AM, Norma Nowak N, Segraves R, Blackwood S, Brown N, Conroy J, Hamilton G, Hindle AK, Huey B, Kimura K, Law S, Myambo K, Palmer J, Ylstra B, Yue JP, Gray JW, Jain AN, Pinkel D, Albertson DG: Assembly of microarrays for genome-wide measurement of DNA copy number by CGH. *Nat Genet* 2001, 29:263–264
 20. Chin S-L, Price JT, Quinn JMW, Miroslavjevic D, Thomas DM: A role for α V integrin subunit in osteoclastogenesis. *Biochem Biophys Res Commun* 2003, 307:1051–1058
 21. Zaidi M, Troen B, Moonga BS, Abe E: Cathepsin K, osteoclastic resorption, and osteoporosis therapy. *J Bone Miner Res* 2001, 16:1747–1749
 22. Sakai D, Tong HS, Minkin C: Osteoclast molecular phenotyping by random cDNA sequencing. *Bone* 1995, 17:111–119
 23. Ikeda F, Nishimura R, Matsubara T, Tanaka S, Inoue J, Reddy SV, Hata K, Yamashita K, Hiraga T, Watanabe T, Kukita T, Yoshioka K, Rao A, Yoneda T: Critical roles of c-Jun signaling in regulation of NFAT family and RANKL-regulated osteoclast differentiation. *J Clin Invest* 2004, 114:475–484
 24. Chen TF, Zhang YL, Xu WL, Li ZQ, Hou B, Wang CL, Fan M, Qian LJ, Zhou RP, Zhang CG: Prokaryotic expression, polyclonal antibody preparation, and sub-cellular localization analysis of Na(+), K(+)-ATPase beta2 subunit. *Protein Expr Purif* 2004, 37:47–52
 25. Zhou H, Kartsogiannis V, Quinn JM, Ly C, Gange C, Elliott J, Ng KW, Gillespie MT: Osteoclast inhibitory lectin, a family of new osteoclast inhibitors. *J Biol Chem* 2002, 277:48808–48815
 26. Bodine PV, Zhao W, Kharode YP, Bex FJ, Lambert AJ, Goad MB, Gaur T, Stein GS, Lian JB, Komm BS: The Wnt antagonist secreted frizzled-related protein-1 is a negative regulator of trabecular bone formation in adult mice. *Mol Endocrinol* 2004, 18:1222–1237
 27. Hausler KD, Horwood NJ, Chuman Y, Fisher JL, Ellis J, Martin TJ, Rubin JS, Gillespie MT: Secreted frizzled-related protein-1 inhibits RANKL-dependent osteoclast formation. *J Bone Miner Res* 2004, 19:1873–1881
 28. Boissy P, Lenhard TR, Kirkegaard T, Peschon JJ, Black RA, Delaisse JM, del Carmen Ovejero M: An assessment of ADAMs in bone cells: absence of TACE activity prevents osteoclast recruitment and the formation of the marrow cavity in developing long bones. *FEBS Lett* 2003, 553:257–261
 29. Bakre MM, Zhu Y, Yin H, Burton DW, Terkeltaub R, Deftos LJ, Varner JA: Parathyroid hormone-related peptide is a naturally occurring, protein kinase A-dependent angiogenesis inhibitor. *Nat Med* 2002, 8:995–1003
 30. Sakuma Y, Li Z, Pilbeam CC, Alander CB, Chikazu D, Kawaguchi H, Raisz LG: Stimulation of cAMP production and cyclooxygenase-2 by prostaglandin E2 and selective prostaglandin receptor agonists in murine osteoblastic cells. *Bone* 2004, 34:827–834
 31. Kong YY, Yoshida H, Sarosi I, Tan HL, Timms E, Capparelli C, Moroney S, Oliveira-dos-Santos AJ, Van G, Itie A, Khoo W, Wakeham A, Dunstan CR, Lacey DL, Mak TW, Boyle WJ, Penninger JM: OPG is a key regulator of osteoclastogenesis, lymphocyte development and lymph-node organogenesis. *Nature* 1999, 397:315–323
 32. Roux S, Orcel P: Bone loss: factors that regulate osteoclast differentiation: an update. *Arthritis Res* 2000, 2:451–456
 33. Carron JA, Wagstaff SC, Gallagher JA, Bowler WB: A CD36-binding peptide from thrombospondin-1 can stimulate resorption by osteoclasts in vitro. *Biochem Biophys Res Commun* 2000, 270:1124–1127
 34. Katagiri M, Hakeda Y, Chikazu D, Ogasawara T, Takato T, Kumegawa M, Nakamura K, Kawaguchi H: Mechanism of stimulation of osteoclastic bone resorption through Gas6/Tyro 3, a receptor tyrosine kinase signaling, in mouse osteoclasts. *J Biol Chem* 2001, 276:7376–7382
 35. Nakamura YS, Hakeda Y, Takakura N, Kameda T, Hamaguchi I, Miyamoto T, Kakudo S, Nakano T, Kumegawa M, Suda T: Tyro 3 receptor tyrosine kinase and its ligand, Gas6, stimulate the function of osteoclasts. *Stem Cells* 1998, 16:229–238
 36. Motyckova G, Weilbaecher KN, Horstmann M, Rieman DJ, Fisher DZ, Fisher DE: Linking osteopetrosis and pycnodysostosis: regulation of cathepsin K expression by the microphthalmia transcription factor family. *Proc Natl Acad Sci USA* 2001, 98:5798–5803
 37. Steingrimsson E, Tessarollo L, Pathak B, Hou L, Arnheiter H, Copeland NG, Jenkins NA: Mitf and Tfe3, two members of the Mitf-Tfe family of bHLH-Zip transcription factors, have important but functionally redundant roles in osteoclast development. *Proc Natl Acad Sci USA* 2002, 99:4477–4482
 38. Sahni M, Zhou XM, Bakiri L, Schlessinger J, Baron R, Levy JB: Identification of a novel 135-kDa Grb2-binding protein in osteoclasts. *J Biol Chem* 1996, 271:33141–33147
 39. Ohsawa Y, Nitatori T, Higuchi S, Kominami E, Uchiyama Y: Lysosomal cysteine and aspartic proteinases, acid phosphatase, and an endogenous cysteine proteinase inhibitor, cystatin-beta, in rat osteoclasts. *J Histochem Cytochem* 1993, 41:1075–1083
 40. Boyle WJ, Simonet WS, Lacey DL: Osteoclast differentiation and activation. *Nature* 2003, 423:337–342
 41. Marie PJ: Fibroblast growth factor signaling controlling osteoblast differentiation. *Gene* 2003, 316:23–32
 42. Yamaguchi A, Komori T, Suda T: Regulation of osteoblast differentiation mediated by bone morphogenetic proteins, hedgehogs, and Cbfa1. *Endocr Rev* 2000, 21:393–411
 43. Yu X, Huang Y, Collin-Osdoby P, Osdoby P: CCR1 chemokines promote the chemotactic recruitment, RANKL development, and motility of osteoclasts and are induced by inflammatory cytokines in osteoblasts. *J Bone Miner Res* 2004, 19:2065–2077
 44. Tian E, Zhan F, Walker R, Rasmussen E, Ma Y, Barlogie B, Shaughnessy JD Jr: The role of the Wnt-signaling antagonist DKK1 in the development of osteolytic lesions in multiple myeloma. *N Engl J Med* 2003, 349:2483–2494
 45. Atkins GJ, Kostakis P, Pan B, Farrugia A, Gronthos S, Evdokiou A, Harrison K, Findlay DM, Zannettino AC: RANKL expression is related to the differentiation state of human osteoblasts. *J Bone Miner Res* 2003, 18:1088–1098
 46. Reid R, Banerjee SS, Sciort R: Giant cell tumour. *WHO Classification of Tumors, Pathology and Genetics, Tumors of Soft Tissue and Bone*. Edited by CDM Fletcher, KK Unni, F Mertens. Lyons, France, IARC Press, 2002, pp 310–312
 47. Li J, Sarosi I, Yan X-Q, Moroney S, Capparelli C, Tan H-L, McCabe S, Elliot R, Scully S, Van G, Kaufman S, Juan S-C, Sun Y, Tarpley J, Martin L, Christensen K, McCabe J, Kostenuik P, Hsu H, Fletcher J, Dunstan CR, Lacey DL, Boyle WJ: RANK is the intrinsic hematopoietic cell surface receptor that controls osteoclastogenesis and regulation of bone mass and calcium metabolism. *Proc Natl Acad Sci USA* 2000, 97:1566–1571
 48. Liu B, Yu SF, Li TJ: Multinucleated giant cells in various forms of giant cell containing lesions of the jaws express features of osteoclasts. *J Oral Pathol Med* 2003, 32:367–375
 49. Yoshida W, Uzuki M, Kurose A, Yoshida M, Nishida J, Shimamura T, Sawai T: Cell characterization of mononuclear and giant cells constituting pigmented villonodular synovitis. *Hum Pathol* 2003, 34:65–73
 50. Huang TS, Green AD, Beattie CW, Das Gupta TK: Monocyte-macrophage lineage of giant cell tumor of bone. Establishment of a multinucleated cell line. *Cancer* 1993, 71:1751–1760
 51. Grano M, Colucci S, De Bellis M, Zigrino P, Argentino L, Zamboni G, Serra M, Scotlandi K, Teti A, Zamboni Zallone A: New model for

- bone resorption study in vitro: human osteoclast-like cells from giant cell tumors of bone. *J Bone Miner Res* 1994, 9:1013–1020
52. Schwartz HS, Dahir GA, Butler MG: Telomere reduction in giant cell tumor of bone and with aging. *Cancer Genet Cytogenet* 1993, 71:132–138
53. Bridge JA, Neff JR, Mouron BJ: Giant cell tumor of bone: chromosomal analysis of 48 specimens and review of the literature. *Cancer Genet Cytogenet* 1992, 58:2–13
54. Panagopoulos I, Mertens F, Domanski HA, Isaksson M, Brosjo O, Gustafson P, Mandahl N: No EWS/FLI1 fusion transcripts in giant-cell tumors of bone. *Int J Cancer* 2001, 93:769–772
55. Sciort R, Dorfman H, Brys P, Dal Cin P, de Wever I, Fletcher CD, Jonson K, Mandahl N, Mertens F, Mitelman F, Rosai J, Rydholm A, Samson I, Tallini G, van den Berghe H, Vanni R, Willen H: Cytogenetic-morphologic correlations in aneurysmal bone cyst, giant cell tumor of bone and combined lesions: a report from the CHAMP study group. *Mod Pathol* 2000, 13:1206–1210
56. Tarkkanen M, Kaipainen A, Karaharju E, Bohling T, Szymanska J, Helio H, Kivioja A, Elomaa I, Knuutila S: Cytogenetic study of 249 consecutive patients examined for a bone tumor. *Cancer Genet Cytogenet* 1993, 68:1–21
57. Zheng MH, Siu P, Papadimitriou JM, Wood DJ, Murch AR: Telomeric fusion is a major cytogenetic aberration of giant cell tumors of bone. *Pathol* 1999, 31:373–378